JOURNAL OF MATERIALS SCIENCE 9 (1974) 18–28

Cyclic stress fatigue and thermal softening failure of a thermoplastic

R. J. CRAWFORD, P. P. BENHAM
Department of Mechanical Engineering, The Queen's University of Belfast

The application of a cyclic stress to a polymeric material causes its temperature to rise with the result that failure may occur by one of two completely different mechanisms. In the first the temperature rises for a time but then stabilizes and allows a conventional crack initiation and propagation process to take place. In the second type of failure the temperature continues to increase and results in a thermal softening failure in the material.

Uniaxial fatigue tests have been carried out on injection moulded acetal co-polymer specimens and the conditions under which each type of failure occurs have been analysed theoretically and empirically. Using relatively simple analysis, indication is given as to how quite acceptable predictions of the observed temperature rises may be made. The effects of mean stress, strain control, as opposed to load control, and cyclic waveform on polymer fatigue behaviour are also indicated.

In addition electron microscopy studies were carried out on the fatigue failures of the injection moulded specimens and these show that microscopic fatigue striations are present and that the size of the defect which has initiated crack growth is typically about 0.13 mm (0.005 in.).

1. Introduction

There are relatively few references [1-6] relating to the fundamentals of fatigue of unreinforced thermoplastics. This is probably because these materials are not often used for engineering components subjected to cyclic stresses. However, that situation is not likely to last and therefore a sound knowledge of fatigue behaviour is desirable. As with the other aspects of the mechanical properties of plastics it is preferable that this data should be presented in a manner similar to that used for metals. It is then only necessary to inform the designer on specific topics which arise from the peculiarities of thermoplastic behaviour. In the case of polymer fatigue the main peculiarity is undoubtedly the thermal aspect of failure.

In contrast to metals, plastics have low thermal conductivity and high damping properties which result in a temperature rise in the specimen during cyclic loading. Depending on the combination of loading parameters the temperature may rise continuously leading to thermal softening failure without crack propagation [3, 4]. Alternatively for certain limits of frequency and cyclic stress the temperature will rise for a period but then achieve a stable value and a conventional form of fatigue crack can be initiated and propagated to complete failure [1, 2].

In this investigation the fatigue behaviour of an engineering thermoplastic is described and the thermal aspect of failure is analysed both theoretically and empirically in an attempt to indicate methods which may be used in deciding what type of failure can be expected under selected loading conditions. In particular the effects of strain control, load control, waveform and mean stress on fatigue behaviour are considered. The morphology of the conventional fatigue fracture of injection moulded specimens is also examined using electron microscopy.

2. Material and apparatus

After consultation with the plastics industry an acetal copolymer was selected as the material to be tested since it is a tough engineering thermoplastic likely to be used in a cyclic stress situation.

Special moulds were designed so that the specimens could be injection moulded under various conditions (single end gated, double end gated, centre gated, rough and polished mould surfaces). Further details of material and moulding operation are given elsewhere [9]. The design of the specimen is illustrated in Fig. 1.

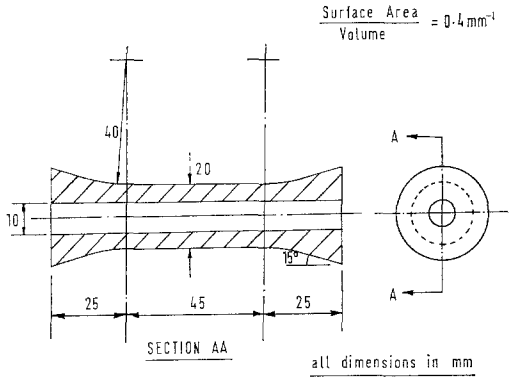

Figure 1 Uniaxial fatigue specimen.

The cross-section had to be adequate to resist buckling in compression, but not too thick so as to make a good quality moulding difficult, hence the tubular cross-section. This had the additional advantages of an extra surface for heat transfer and the ability to accommodate at some future date internal pressure, some coolant or an aggressive environment. The parallel length of the specimen was designed to accommodate an extensometer.

The fatigue tests were carried out on a push-pull hydraulic servo-controlled machine having load ranges of 5 and 20 kN, extension ranges of 0.25, 0.5 and 2.5 mm and a frequency range from 0.1 to 100 Hz. Further details of the machine and extensometry are given elsewhere [9].

The surface temperature rise of the specimens during cyclic loading was recorded using an infra-red radiation thermometer.

3. Results and discussion

As described in the Introduction the application of a cyclic stress to a thermoplastic results in a temperature rise which is strongly dependent on the cyclic frequency and the applied stress. As would be expected from the visco-elastic behaviour of polymers the rise is also dependent on the mode of control and so in Fig. 2 the nature of the temperature rise is shown for fully reversed cycling at a frequency of 5 Hz under load control.

At the lower stresses the temperature of the material rises but then stabilizes and allows a conventional type of fatigue failure to occur. If a higher stress amplitude is used then there is a higher stable temperature rise until eventually a particular stress amplitude is reached where the temperature, instead of stabilizing, continues to increase. This results in a thermal failure in the material through a drastic drop in modulus. The way in which this behaviour effects the fatigue properties of the material is shown in Fig. 3.

At 5 Hz a thermal runaway failure, denoted by T, occurs if the stress amplitude is above 21.6 MN m^{-2} whereas a conventional fatigue failure occurs if the stress is below this level. If the frequency is reduced to 1.67 Hz then thermal failures only occur for stress amplitudes greater than 27.8 MN m^{-2}. From Fig. 3 it may be observed that for this material there is very little frequency effect on the fatigue failures whereas there is a large frequency effect on the thermal failures. Thus a component to be stressed at $\pm$ 18 MN m^{-2} would show little difference in cycles to failure if it was cycled at 5 Hz instead of 1.67 Hz whereas if it was to be stressed at $\pm$ 25 MN m^{-2} then there would be a large difference in life depending on which frequency was used.

3.1. Analysis of temperature rise during fatigue

Since the temperature rise which occurs during polymer fatigue can, depending on the conditions, produce a short life thermal fatigue failure, it is important for the designer to be able to estimate what combinations of loading parameters are likely to produce such a failure. In principle this is not a difficult problem in that it basically involves the heat transfer from the component to the surroundings. However, the accuracy of the temperature predictions will clearly depend on the accuracy with which the energy dissipation and various heat transfer processes can be defined. As might be expected this is where the difficulties can arise but to indicate how the problem might be attempted the thermal aspect of failure encountered in this investigation has been analysed. This shows how an approximation to the temperature rise may be made, while awaiting a more rigorous solution, to the heat transfer problem.

When a linear visco-elastic material is sub-

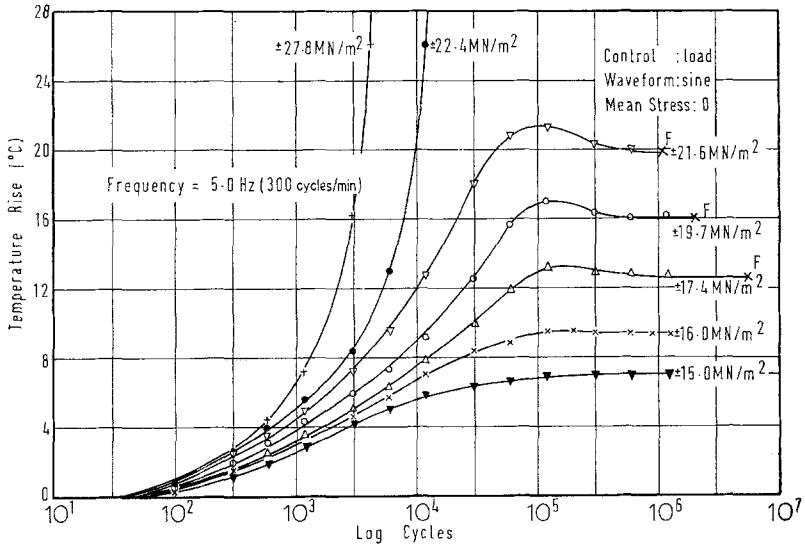

Figure 2 Specimen temperature rise during fatigue.

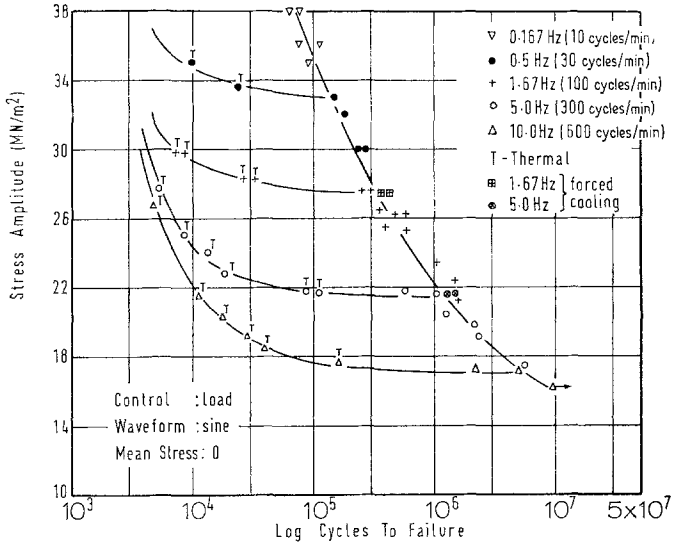

Figure 3 Fatigue and thermal failure curves.

jected to a sinusoidal variation of stress, the strain lags behind the stress by an angle δ. The stress, σ, and the strain, ϵ, may therefore be represented by rotating vectors of the form

$$\epsilon = \epsilon_a \sin \omega t \qquad (1)$$

$$\sigma = \sigma_a \sin (\omega t + \delta) \qquad (2)$$

where ω is the angular frequency, t is time and the subscript "a" refers to amplitude.

Now the total energy input per unit volume, W, is given by

$$W = \int \sigma . d\epsilon \ . \qquad (3)$$

So from Equations 1 and 2

$$W = \int \sigma_a \, \epsilon_a \, \omega \sin (\omega t + \delta) . \cos \omega t . dt .$$

The solution of this integral [7] indicates that the input energy consists of two parts. The first of these is recoverable energy but the remainder appears as heat and is effectively lost.

Expressing this non-recoverable energy per unit volume per cycle as W'', then

$$W' = \pi \sigma_a \epsilon_a \sin \delta.$$

If the volume of the material is V and the cyclic frequency is f then the work dissipated as heat per unit time, Q, is given by

$$Q = \pi V f \sigma_a \epsilon_a \sin \delta. \quad (4)$$

Some of this heat is lost to the surroundings, Q_L, so the total heat per unit time, Q_T, is given by

$$Q_T = Q - Q_L. \quad (5)$$

Under normal conditions the major contributor to the heat transfer will be free convection in which case

$$Q_L = hA\theta$$

where h = heat transfer coefficient, A = surface area and θ = temperature difference between specimen surface and surroundings.

To be more specific, for the hollow cylindrical shape of specimen used in the fatigue tests the heat transfer is given by

$$\begin{aligned} Q_L &= \{h_o A_o \theta + h_i A_i \theta\} \\ &= \left\{h_o \left(\frac{2}{3} A\right)\theta + h_i \left(\frac{1}{3} A\right) \theta\right\} \\ &= A\theta \left\{\frac{2}{3} h_o + \frac{1}{3} h_i\right\} \end{aligned}$$

where the subscripts "i" and "o" refer to the inner and outer surfaces of the specimen.

So in Equation 5

$$Q_T = \pi V f \sigma_a \epsilon_a \sin \delta - A\theta \left\{\frac{2}{3} h_o + \frac{1}{3} h_i\right\}$$

but also

$$Q_T = V \rho C_p \frac{d\bar{\theta}}{dt}$$

where ρ = density of the material, C_p = specific heat, $\bar{\theta}$ = temperature of specimen.

Therefore

$$\frac{d\bar{\theta}}{dt} = \frac{\pi f \sigma_a \epsilon_a}{\rho C_p} \sin \delta - \frac{A\theta}{V \rho C_p} \left\{\frac{2}{3} h_o + \frac{1}{3} h_i\right\}$$

or

$$\frac{d\bar{\theta}}{dt} = \frac{\pi f \sigma_a^2}{\rho C_p} \cdot \frac{\sin \delta}{E} - \frac{\beta \theta}{\rho C_p} \left\{\frac{2}{3} h_o + \frac{1}{3} h_i\right\} \quad (6)$$

where $\beta = A/V$ (surface area to volume ratio), $E = \sigma_a/\epsilon_a$ (modulus).

Owing to the low thermal conductivity of the material the temperature within the wall of the specimen will be greater than the temperature at the surface. This means that in Equation 6 $\bar{\theta}$ is not equal to θ. However, as a first approximation they may be assumed to be the same and indeed by estimating the steady state radial heat conduction through a hollow cylinder from the standard equation, it can be shown that this is an acceptable assumption to make [8]. For example, when the surface temperature is 20°C it can be shown that the centre of the specimen wall is 2.7°C higher and when the temperature of the surface is 5°C, the difference is only 0.5°C.

Equation 6 may therefore be rewritten as

$$\frac{d\theta}{dt} = R - S\theta \cdot$$

If R and S are assumed to be independent of temperature then this simple differential equation has a solution of the form

$$\theta = \frac{R}{S}(1 - e^{-St})$$

which indicates an exponential rise of temperature to a value of

$$\theta_{equil} = R/S.$$

This is a simple relationship which would obviously be very useful but unfortunately a few calculations with it show that the temperatures which it predicts are not very accurate. The reason for this is that the temperature dependence of R and S cannot be ignored. S depends on temperature because of h and this dependence must be determined from published data which refers as closely as possible to the component shape [10, 11]. R depends on temperature because of sin δ and E and this dependence must again be determined from published data or, as in this case, from direct experimentation on the material. In these tests sin δ and E were recorded directly during the fatigue tests by means of the extensometry attached to the specimens. The variation of sin δ/E with temperature at several stress amplitudes is shown in Fig. 4.

Once the temperature dependence of h, sin δ and E had been established this was substituted in Equation 6. Unfortunately, however, because the heat transfer coefficient, h_o, was related to temperature, θ, by a power of 0.25 it was not possible to get an explicit solution of the differential equation for θ in terms of the other parameters. It was therefore necessary to use either a graphical solution or an iterative solution involving a computer.

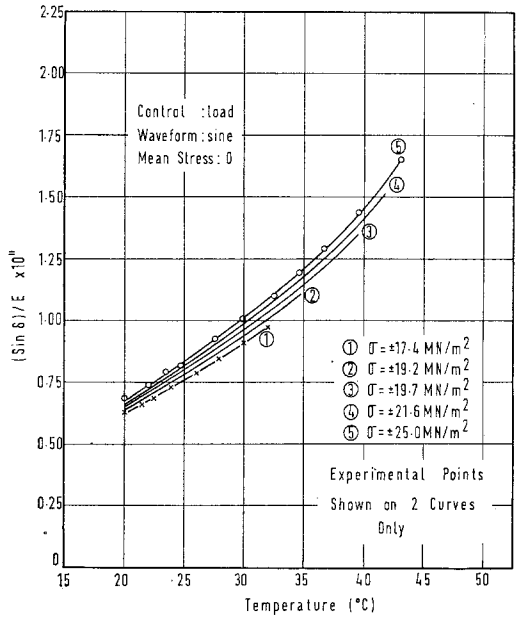

Figure 4 Variation of (sin δ)/E with temperature at 5 Hz.

3.1.1. Graphical solution

In this solution, once the temperature dependence of the heat transfer coefficients had been included in Equation 6 the heat transfer term was plotted against the temperature rise, θ, as shown in Fig. 5. Then superimposed on this a second graph for the energy dissipation was plotted against θ for a particular stress amplitude and frequency and using the values of (sin δ)/E from Fig. 4. From Equation 6 it may be seen that the point at which the two lines intersect gives the value of θ necessary to make the rate of temperature rise zero. This is therefore the equilibrium temperature rise.

If a higher stress amplitude is used at the same frequency then a higher stable temperature rise is predicted until eventually at some value of stress amplitude the two lines no longer intersect. This then defines the cross over stress level required to produce thermal failures. Note also the effect of increasing the surface area to volume ratio, β, is to rotate the heat transfer line anti-clockwise, thus predicting a lower temperature rise at any particular stress amplitude and frequency.

3.1.2. Computer solution

In the iterative solution the temperature dependence of (sin δ)/E from Fig. 4 was approximated by a straight line of the form ($a\theta + b$). A computer programme was then written which enabled the parameters σ_a, f, ρ, C_p, β etc. to be read in and the values of θ examined to make the rate of temperature rise, in Equation 6, zero. If the solution did not converge towards zero then a thermal runaway failure was indicated. Fig. 6 shows the temperature predictions given by each method at two frequencies along with the actual

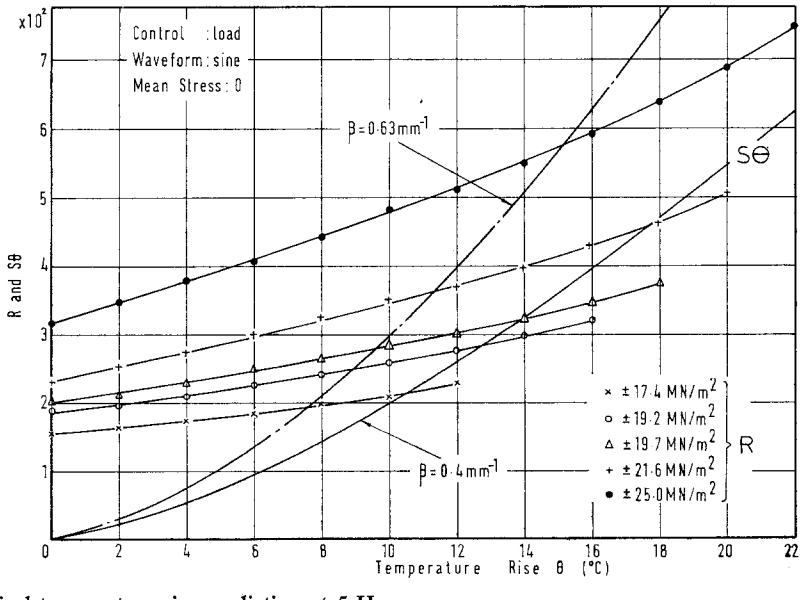

Figure 5 Graphical temperature rise prediction at 5 Hz.

temperature rises as recorded by the infra-red radiation thermometer. It can be seen from this that quite acceptable predictions of temperature rise were possible using these relatively simple techniques.

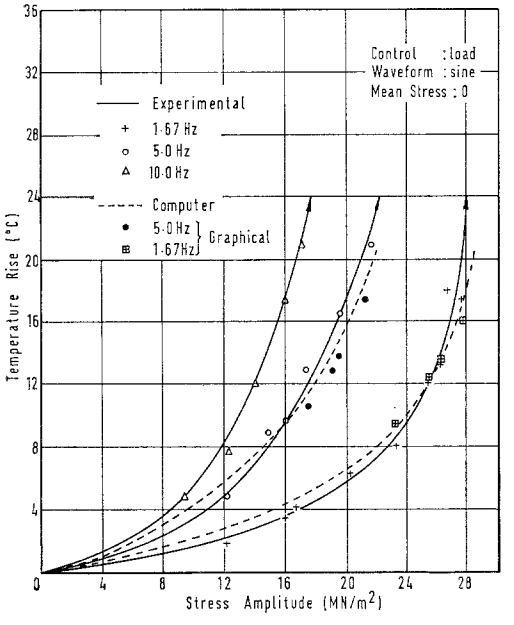

Figure 6 Equilibrium temperature rise against stress amplitude.

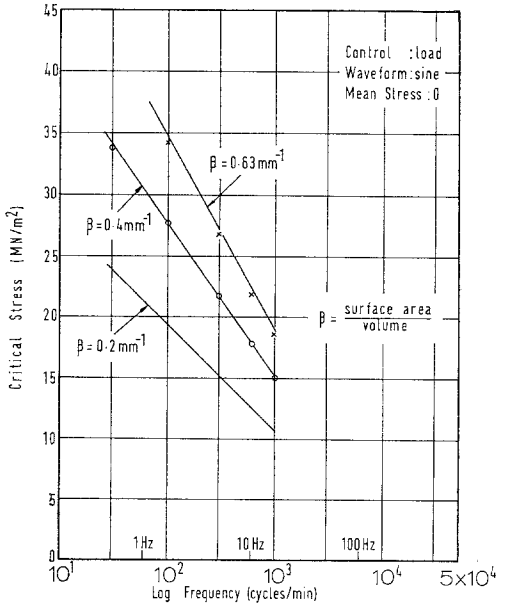

Figure 7 Critical thermal softening stress against frequency.

3.2. Empirical approach

When the cross-over stress amplitude, σ_c, required to just produce a thermal failure at any frequency was plotted against the logarithm of frequency it was found that for any particular surface area to volume ratio a straight line relationship existed up to at least 20 Hz. This is shown in Fig. 7 and the relationship can be represented by an equation of the form

$$\sigma_c = \{X - Y \log_{10} f\} \sqrt{\beta}$$

where $X = 47.3$ and $Y = 19.8$ when σ_c is in MN m^{-2}, β in mm^{-1} and f in Hz.

The numbers quoted will only apply to the acetal co-polymer tested and at present the existence of such a relationship is being examined for several other materials. Already it has been confirmed to exist for polymethylmethacrylate up to 20 Hz where in this case $X = 56.2$ and $Y = 30.8$ when σ_c, β and f have the units as before.

If this relationship does exist for a number of materials it could be very useful in that only a small number of short term tests on the material are necessary to obtain the constants X and Y. These can then be used to determine the combinations of stress, frequency and specimen size to produce or avoid thermal failures over a much wider range of these parameters. The advantages of this would be in the design of a component or in the setting up of a polymer fatigue test programme on a new material where the test conditions, specimen dimensions, etc. could be selected in a way which would optimize the tests in terms of testing time and information received.

3.3. Effect of strain control

The results described so far have all been for load control. Fig. 8 shows that during these tests the strain range increases mainly due to the drop in modulus caused by the increase in temperature of the specimens during cyclic loading.

If, however, the strain is controlled then the drop in modulus causes the stress level to decrease as shown in Fig. 9. There is a basic difference between the two modes of control therefore, in that the drop in modulus during load control causes an increases in the energy dissipation whereas in strain control the drop in modulus causes a decrease in energy dissipation. This means that in the latter case there is a self-stabilizing mechanism with the result that there are no thermal runaway failures under strain

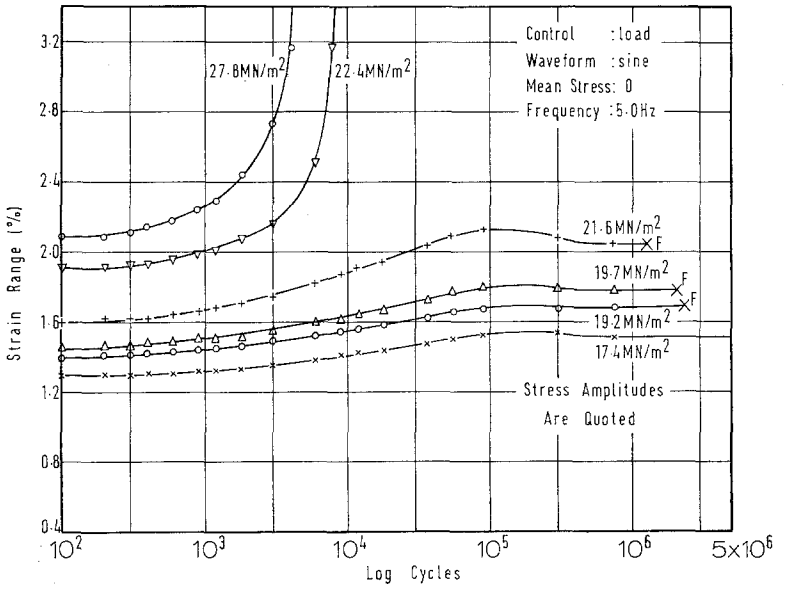

Figure 8 Variation of strain range during fatigue.

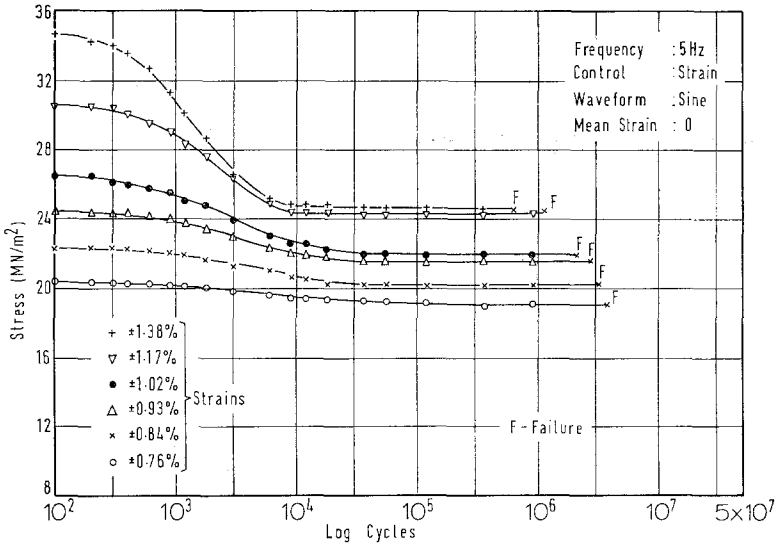

Figure 9 Decrease in stress during strain cycling.

control. The temperature rise curves are similar to those in Fig. 2 with the exception that the temperature rise always stabilizes. Using the same methods described in the earlier section for load control, good predictions of these temperature rises have been made [8].

The fatigue data cannot be plotted as initial stress amplitude against cycles to failure, N, because as shown in Fig. 9 this stress is only maintained on the specimen for a very short time. The usual procedure is to plot strain against $\log_{10} N$ and this gives the conventional shape of fatigue curve. However, in order to get a better comparison with load control data it is suggested that since the decreasing stress amplitude stabilizes after a period of time representing

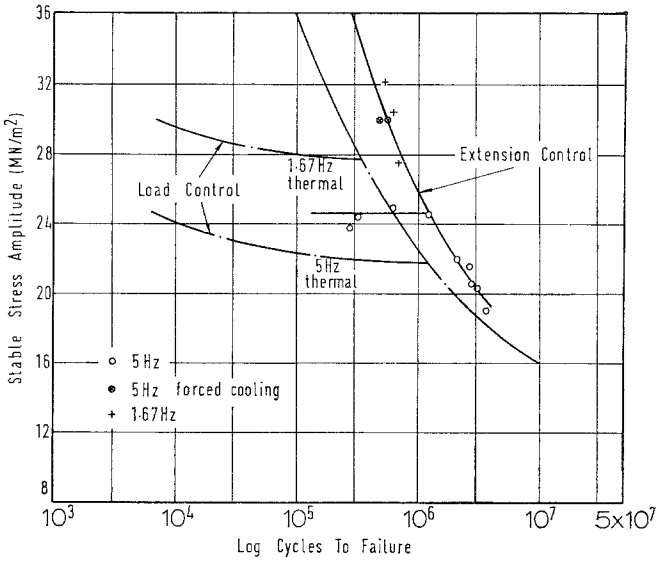

Figure 10 Fatigue curve for strain control cycling.

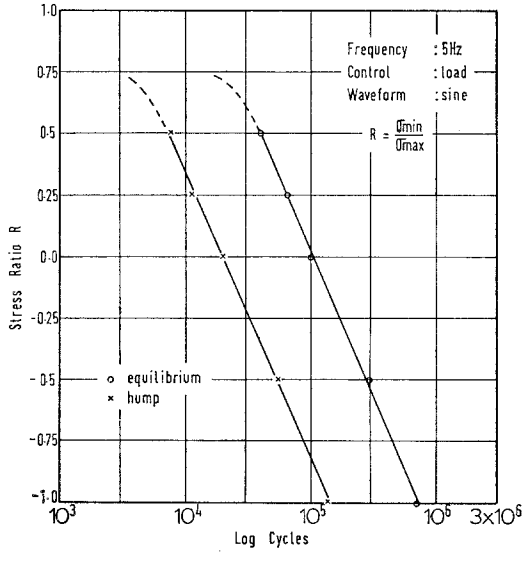

Figure 11 Cycles to reach thermal equilibrium as a function of stress ratio.

approximately 1% of the total life, then it is reasonable to plot the reduced stable stress against $\log_{10} N$. This produces an interesting fatigue curve in that at any frequency, although there are no thermal lines, there is an upper limit for the reduced stable stress. At that frequency it is not possible to have a higher reduced stable stress irrespective of the initial applied stress, due to the large drop in modulus which occurs. It is only possible to get higher reduced stable stresses by decreasing the frequency. The remainder of the fatigue curve takes the conventional shape and when this is compared in Fig. 10 with the curve produced by load control, it would suggest that failure is more strain-dependent than stress-dependent.

3.4. Effect of mean stress

A detailed discussion of the effect of a mean stress on the fatigue of polymers will be given elsewhere [9] and so only the thermal aspect will be referred to here. In general terms the presence of a mean stress under load control does not affect. the shape of the temperature rise characteristics. The temperature increases during cycling and depending on the test conditions may stabilize to permit a conventional fatigue mechanism or alternatively may continue to increase, resulting in a thermal runaway failure. Defining the stress ratio, R, as $\sigma_{min}/\sigma_{max}$ then, as R increases from -1 (fully reversed) to 0 (repeated tension) the amplitude of stress required to just produce a thermal failure at any frequency, decreases. In connection with this it is interesting that the number of cycles required for the temperature to stabilize is dependent on the stress ratio, R, as shown in Fig. 11. This dependence apparently applies for both the equilibrium steadying off of temperature and the characteristic "hump" observed on the temperature rise curves. Once again the temperature prediction techniques

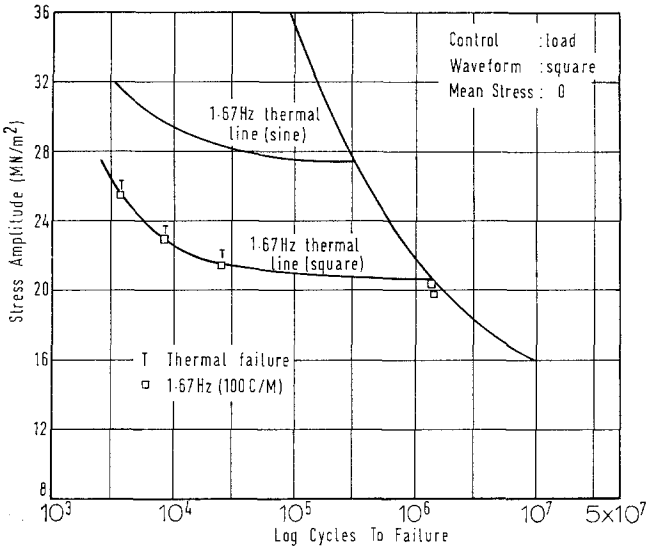

Figure 12 Fatigue curve for square waveform.

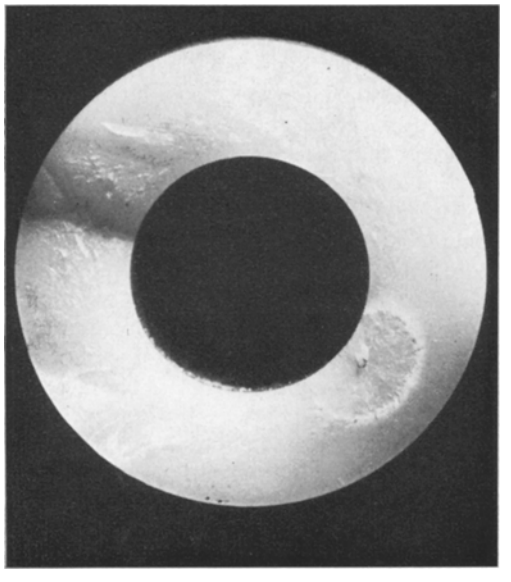

Figure 13 Fatigue failure as a result of crack growth.

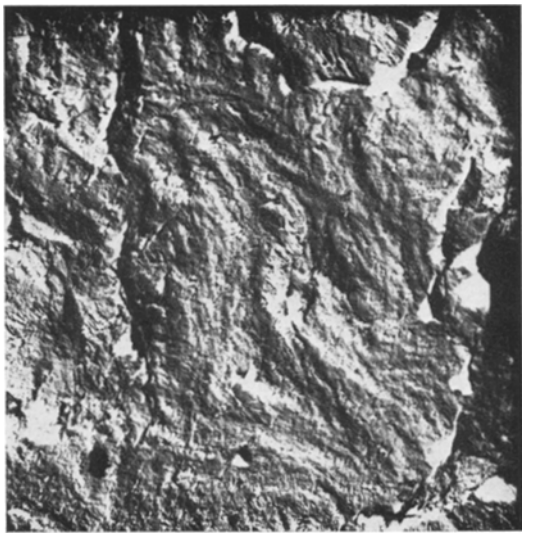

Figure 14 Electron micrograph of area inside ellipse (× 1400).

described earlier may be used when a mean stress is present [8].

3.5. Effect of waveform

A comparison has been made between the use of square as opposed to sinusoidal waveforms, mainly as regards thermal failures because of the time consumed in producing conventional fatigue failures (see Fig. 12). In this figure it may be seen that there is a pronounced effect as a result of the greater energy dissipation during square wave cycling. In effect the cross over stress amplitude is reduced from 27.8 MN m^{-2} at 1.67 Hz using a sine wave to 21.5 MN m^{-2} at 1.67 Hz using a square wave. From the few tests performed which produced a conventional

fatigue failure no difference in fatigue life was observed between the two waveforms.

3.6. Fracture morphology

If attention is now turned towards the conventional fatigue failures the first interesting feature is that when no notch was present in the specimens failure initiated from within the wall thickness and not from the surface, as would normally occur in metals. Macroscopic examination of the fracture surface showed that around the point from which crack growth had initiated there was a relatively rough region. This was bounded by a thin white ellipse beyond which the surface was very smooth with step-like features in regions remote from the elliptical region. Directly opposite to the crack initiation area there was a radial step across the specimen wall where the two crack fronts departing from each side of the ellipse had come together. This is shown in Fig. 13 and both halves of a fractured specimen were similar. Some specimen fractures also indicated that crack growth was occurring on several planes along the specimen.

Using a single stage replica technique, electron micrographs were taken of the areas inside and outside the ellipse. Figs. 14 and 15 give a comparison of these two areas and indicates the very smooth nature of the area outside the ellipse. A macroscopic examination of the crack propagation area inside the ellipse did not show

Figure 15 Electron micrograph of area outside ellipse (× 1400).

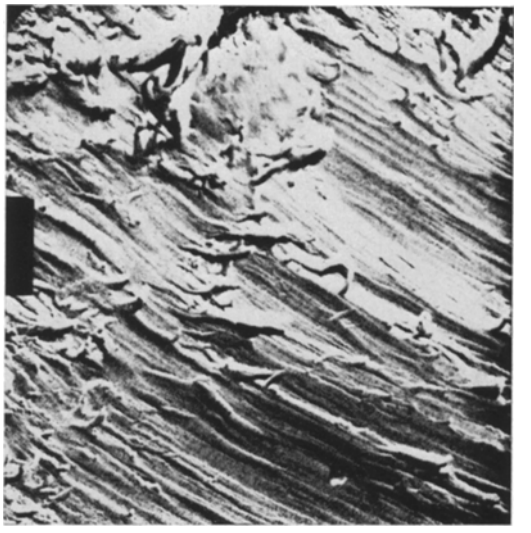

Figure 16 Electron micrograph of area inside ellipse (× 14000).

Figure 17 Scanning electron micrograph of fatigue failure initiator (× 98).

any fatigue characteristics such as striations, but at a magnification of 1400, in Fig. 14, there is some evidence to suggest that these may be present on a microscopic scale. Higher magnification of this area (Fig. 16) does in fact reveal that ripples or striations are present but they are discontinuous and random in direction. Generally it appears that a series of these ripples are initiated from a microscopic step or recess on the surface and then proceed in a certain direc-

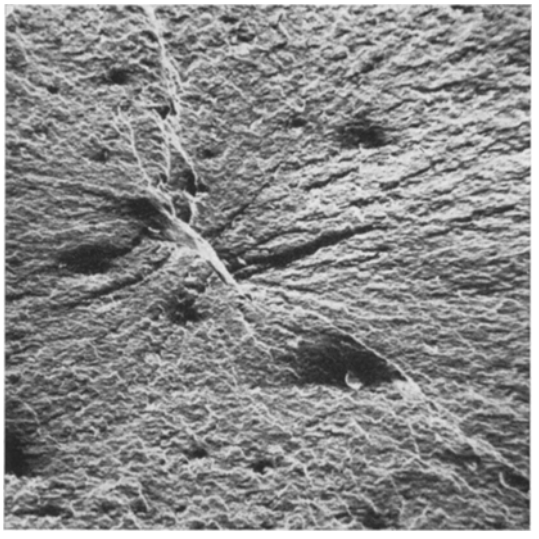

Figure 18 Scanning electron micrograph of fatigue failure initiator (× 98).

tion until arrested by a similar step or ridge. This may cause that particular series of striations to stop completely or alternatively cause them to move off in a different direction.

Figs. 17 and 18 are scanning electron micrographs of the type of defect within the wall thickness which has initiated the fatigue failure. In Fig. 17 this takes the form of an inclusion whereas in Fig. 18 it is a small pit or void. In both cases the greatest dimension of the defect is about 0.13 mm (0.005 in.).

4. Conclusions

1. Cyclical uniaxial stressing of an acetal copolymer results in two mechanisms of failure. One is the result of continuous temperature rise leading to thermal softening failure and is markedly frequency-dependent. The other occurs as a result of a conventional crack initiation and propagation mechanism and is largely independent of frequency.

2. The rate of temperature rise during cyclic loading can be predicted analytically by considering the energy dissipation in and heat transfer from the material. This enables predictions of the highest stress amplitude which will lead to fatigue fracture rather than thermal softening.

3. An empirical relationship between this highest stress amplitude, frequency and surface area to volume ratio was found to exist and this can also be used in selecting conditions to avoid thermal softening failures.

4. If strain control as opposed to load control is used during uniaxial cycling then no thermal runaway failures are produced. Instead the initial stress level decreases and then stabilizes at a reduced level after a time equivalent to about 1% of the total life.

5. The presence of a mean stress under load control can, depending on the loading conditions, produce thermal softening failures and for any particular endurance increasing the mean stress reduces the allowable range of stress.

6. When a mean stress is present the number of cycles required for thermal equilibrium to occur is dependent on the stress ratio ($\sigma_{min}/\sigma_{max}$).

7. The use of a square waveform as opposed to a sinusoidal waveform results in much greater energy dissipation in the material.

8. Fatigue cracks do not develop from the polished free surface but from small internal flaws developed during injection moulding. The size of these flaws is typically about 0.13 mm (0.005 in.).

9. Fatigue striations are present on a microscopic scale on the crack growth area of fracture.

Acknowledgements

The authors are most grateful to ICI Plastics Division (K. Gotham, P. Vincent and S. Turner) for their comments during discussions on the work. The Company also generously provided the special moulds and produced the specimens in the required conditions. Financial support for the equipment was obtained from SRC.

References

1. E. H. ANDREWS, "Testing of Polymers" (Edited by W. E. Brown) Vol. 4 (Wiley, New York, 1968) p. 237.
2. K. V. GOTHAM, *Plastics and Polymers* **37** (1969), 309.
3. M. N. RIDDELL, G. P. KOO and J. L. O'TOOLE, *Polymer Eng. and Sci.* (1966) 363.
4. I. CONSTABLE, J. G. WILLIAMS and D. J. BURNS, *J. Mech. Eng. Sci.* **12** (1970) 20.
5. W. J. PLUMBRIDGE, *J. Mater. Sci.* **7** (1972) 939.
6. B. TOMKINS and W. D. BIGGS, *ibid* **4** (1969) 532.
7. K. OBERBACH, *Kunststoffe* **59** (1969) 37.
8. R. J. CRAWFORD, Ph.D. Thesis (1973), Queen's University, Belfast.
9. P. P. BENHAM and R. J. CRAWFORD, PI Conference "Designing to Avoid Mechanical Failure", Paper 9, January, 1973.
10. M. FISHENDEN and O. SAUNDERS, "Heat transfer" (Oxford University Press, 1950).
11. A. J. EDE, "An Introduction to Heat Transfer Principles and Calculations" (Pergamon Press, Oxford, 1967).

Received 13 July and accepted 18 July 1973.